Inorganic Chemistry

Article

pubs.acs.org/IC

Synthesis and Structural Characterization of Inorganic-Organic-Inorganic Hybrids of Dipalladium-Substituted γ-Keggin Silicodecatungstates

Tomohisa Hirano, Kazuhiro Uehara, Sayaka Uchida,† Mitsuhiro Hibino, Keigo Kamata, and Noritaka Mizuno*

Department of Applied Chemistry, School of Engineering, The University of Tokyo, 7-3-1 Hongo, Bunkyo-ku, Tokyo 113-8656, Japan

Supporting Information

ABSTRACT: Three inorganic-organic-inorganic hybrids of dipalladium-substituted γ-Keggin silicodecatungstates with organic linkers of different lengths, $TBA_8[\{(\gamma\text{-}H_2SiW_{10}O_{36}Pd_2)(O_2C(CH_2)_nCO_2)\}_2]$ (n = 1 (**II**), 3 (**III**), and 5 (**IV**), TBA = $[(n\text{-}C_4H_9)_4N]^+$), were synthesized by exchange of the acetate ligands in $TBA_4[\gamma\text{-}H_2SiW_{10}O_{36}Pd_2(OAc)_2]$ ($\mathbf{I_{TBA}}$) with malonic, glutaric, and pimelic acids, respectively. The X-ray crystallographic analysis of **II**, $\mathbf{III_A}$ ($\mathbf{III_A}$: **III** with DCE, DCE = 1,2-dichloroethane), and $\mathbf{IV_A}$ ($\mathbf{IV_A}$: **IV** with 10DCE) revealed that the anion parts of **II**, $\mathbf{III_A}$, and $\mathbf{IV_A}$ were inorganic-organic-inorganic hybrids composed of two dipalladium-substituted γ-Keggin silicodecatungstates connected by two dicarboxylate ligands. In the crystal structure of $\mathbf{IV_A}$, 10 DCE molecules per polyanion were present in the vicinity of polyanions. Compound $\mathbf{IV_B}$ ($\mathbf{IV_B}$: **IV** with 0.2DCE) was obtained by the evacuation of $\mathbf{IV_A}$. The DCE sorption−desorption isotherms of $\mathbf{IV_B}$ showed that the amount of DCE sorbed was saturated at 10.5 mol mol^{-1}, of which the amount was close to that (10 mol mol^{-1}) of crystallographically assigned DCE molecules. In the DCE sorption−desorption isotherms, a low-pressure hysteresis was observed probably because of hydrogen-bonding interaction between DCE molecules and polyanions. The powder X-ray diffraction (XRD) pattern of $\mathbf{IV_A}$ changed with decrease in the relative DCE vapor pressure to form $\mathbf{IV_C}$ ($\mathbf{IV_C}$: **IV** with 0.7DCE) at P/P_0 = 0.0. The in situ powder XRD study showed reversible structure transformation between $\mathbf{IV_A}$ and $\mathbf{IV_C}$ driven by the sorption−desorption of DCE.

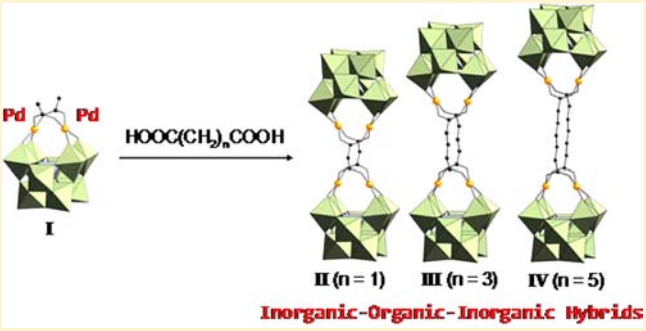

INTRODUCTION

Inorganic-organic hybrids have drawn enormous attention because of their promising applications to optical and electronic materials, solid electrolytes, catalysts, and separation materials.[1] The rational design of structures and functionalities of hybrids requires fine-tuning of both organic and inorganic components. In this context, polyoxometalates (POMs, anionic metal−oxygen clusters) are very attractive building blocks for functional hybrids because their physical and chemical properties can be controlled at the atomic and molecular levels and POM-based hybrids provide additional and/or enhanced functions derived from synergistic effects between POMs and organic components.[2] Therefore, there have been increasing efforts toward synthesis of various POM-based hybrids with unique electronic, catalytic, redox, and photonic properties.[3]

POM-based inorganic-organic-inorganic hybrids are synthesized by connecting two POMs by organic linkers.[4] Some unique behaviors of the hybrids have been reported: For example, two hydrophilic trivanadium-substituted Dawson POMs connected by hydrophobic bis(trisalkoxo) linkers exhibit self-assembly behaviors, leading to the formation of a POM-alkylammonium cation bilayer-type structure with one-dimensional (1D) channels in the solid state and a vesicle in the solution state.[4a−c] The hybrids composed of two Lindqvist POMs and π-conjugated organic linkers form 1D zigzag infinite chains due to hydrogen-bonding interaction between hybrids in crystal structures.[4f] However, the synthesis and structural characterization of the hybrids, especially composed of Keggin POMs, have rarely been reported. While there are several synthetic methodologies of these hybrids, ligand exchange of transition-metal substituted POMs (TMSPs) has been less used because of difficulty in the synthesis of stable TMSPs with exchangeable ligands.[2c,4] We envisaged that TMSPs with acetate ligands likely act as good precursors for TMSP-based hybrids because (i) acetate ligands show flexible and diverse coordination modes and (ii) there are various kinds of TMSPs with acetate ligand(s) (Table S1 in the Supporting Information).[5]

Received: December 9, 2012
Published: February 11, 2013

   dx.doi.org/10.1021/ic302703k | Inorg. Chem. 2013, 52, 2662−2670

Table 1. Crystallographic Data for II, III_A, and IV_A

	II	III_A	IV_A
formula	$C_{134}N_8O_{80}Pd_4Si_2W_{20}$	$C_{138}Cl_2N_8O_{80}Pd_4Si_2W_{20}$	$C_{162}Cl_{20}N_8O_{80}Pd_4Si_2W_{20}$
fw	7160.2	7303.2	8205.5
crystal system	monoclinic	monoclinic	orthorhombic
space group	$P2_1/a$ (No. 14)	$P2_1/a$ (No. 14)	$Pbca$ (No. 61)
a (Å)	17.0069(2)	30.4333(2)	29.4889(9)
b (Å)	24.7919(3)	26.6216(2)	28.5880(6)
c (Å)	27.3714(4)	31.2528(2)	29.7538(8)
α (deg)	90.0000	90.0000	90.0000
β (deg)	92.6080(10)	112.7141(3)	90.0000
γ (deg)	90.0000	90.0000	90.0000
V (Å^3)	11528.7(3)	23356.7(3)	25083.3(11)
Z	2	4	4
temp. (K)	183	153	123
GOF	1.112	1.163	1.052
$R1$ [$I > 2\sigma(I)$]	0.0726	0.0809	0.103
$wR2$ [$I > 2\sigma(I)$]	0.2427	0.2746	0.3242

Table 2. Selected Bond Lengths (Å) and Angles (deg) for II, III_A, IV_A, and I_{TPeA}

	II	III_A (anion 1)[a]	III_A (anion 2)[a]	IV_A	I_{TPeA}[b]
			Bond Length		
Pd1(3)−O1(41)	1.987(8)	1.995(8)	1.989(10)	1.942(18)	1.987(11)
Pd1(3)−O2(42)	1.962(9)	1.989(9)	2.012(10)	1.984(18)	1.984(12)
Pd1(3)−O37(77)	2.011(9)	1.978(10)	2.014(10)	2.001(18)	2.011(13)
Pd1(3)−O38(78)	1.992(10)	1.995(9)	1.997(10)	1.973(19)	2.027(15)
Pd2(4)−O3(43)	1.985(8)	1.990(11)	1.992(9)	1.955(17)	2.002(10)
Pd2(4)−O4(44)	1.983(8)	1.994(10)	1.977(9)	1.974(19)	1.984(12)
Pd2(4)−O39(79)	1.996(9)	1.979(10)	2.018(10)	2.010(20)	1.991(13)
Pd2(4)−O40(80)	2.004(9)	2.002(11)	2.009(8)	2.004(19)	2.002(14)
			Bond Angle		
O1(41)−Pd1(3)−O2(42)	90.5(4)	90.2(4)	91.4(4)	90.4(7)	89.6(5)
O1(41)−Pd1(3)−O37(77)	90.3(3)	89.1(4)	85.1(4)	86.7(8)	89.1(5)
O2(42)−Pd1(3)−O38(78)	87.5(4)	87.9(4)	90.3(5)	88.8(8)	88.4(6)
O37(77)−Pd1(3)−O38(78)	90.2(4)	91.3(5)	91.5(5)	92.8(8)	91.3(6)
O3(43)−Pd2(4)−O4(44)	89.7(4)	90.5(4)	89.9(4)	90.1(8)	90.5(5)
O3(43)−Pd2(4)−O39(79)	87.6(4)	87.7(4)	89.4(4)	88.9(8)	85.9(5)
O4(44)−Pd2(4)−O40(80)	88.4(4)	87.7(5)	90.4(4)	85.5(8)	89.5(6)
O39(79)−Pd2(4)−O40(80)	91.8(5)	92.8(5)	88.7(4)	93.5(9)	92.2(6)

[a]Anion **1** and anion **2** are crystallographically independent molecules. [b]Ref 6.

Recently, we have reported the synthesis and catalytic application of a dipalladium-substituted γ-Keggin silicodecatungstate with acetate ligands, $TBA_4[\gamma\text{-}H_2SiW_{10}O_{36}Pd_2(OAc)_2]$ ($\mathbf{I_{TBA}}$, TBA = $[(n\text{-}C_4H_9)_4N]^+$).[6] The acetate ligands are eliminated by the reaction of $\mathbf{I_{TBA}}$ with water. Because of lability of the acetate ligands in $\mathbf{I_{TBA}}$, we expect that $\mathbf{I_{TBA}}$ can be used as an inorganic component of POM-based hybrids. Herein, we report the successful synthesis and structural characterization of inorganic-organic-inorganic hybrids of dipalladium-substituted γ-Keggin silicodecatungstates with dicarboxylate ligands, $TBA_8[\{(\gamma\text{-}H_2SiW_{10}O_{36}Pd_2)(O_2C\text{-}(CH_2)_nCO_2)\}_2]$ (n = 1 (**II**), 3 (**III**), and 5 (**IV**)). In addition, the reversible structure transformation of **IV** during sorption−desorption of DCE (DCE = 1,2-dichloroethane) is revealed by in situ powder X-ray diffraction (XRD) measurements.

RESULTS AND DISCUSSION

Synthesis and Characterization of Inorganic-Organic-Inorganic Hybrids. Three kinds of TBA salts of inorganic-organic-inorganic hybrids **II**, **III**, and **IV**, were synthesized by the reactions of $\mathbf{I_{TBA}}$ with 1 equiv of malonic, glutaric, and pimelic acids, respectively, in a mixed solvent of acetone and water. The molecular structures of **II**, **III**, and **IV** were successfully determined by X-ray crystallography. The crystallographic data and selected bond lengths and angles are summarized in Tables 1 and 2, respectively. The X-ray crystallographic analysis of **II**, $\mathbf{III_A}$ ($\mathbf{III_A}$: **III** with DCE), and $\mathbf{IV_A}$ ($\mathbf{IV_A}$: **IV** with 10DCE) show that the anion parts of **II**, $\mathbf{III_A}$, and $\mathbf{IV_A}$ are inorganic-organic-inorganic hybrids of dipalladium-substituted γ-Keggin silicodecatungstates connected by two malonate, glutarate, and pimelate ligands, respectively (Figure 1).[7] For all compounds, eight TBA cations per polyanion could crystallographically be assigned, in accord with the results of elemental analysis. In the crystal lattice of $\mathbf{IV_A}$, 10 DCE molecules per polyanion (ca. 21% of the unit cell volume) were observed in the voids surrounded by polyanions and TBA cations. Similarly to **IV** the solvent accessible voids in the crystal lattices of **II** and $\mathbf{III_A}$ were 19% and 19% of the unit cell volumes, respectively, and large, suggesting the existence of the solvent molecules in these voids, while all positions of the

dx.doi.org/10.1021/ic302703k | Inorg. Chem. 2013, 52, 2662−2670

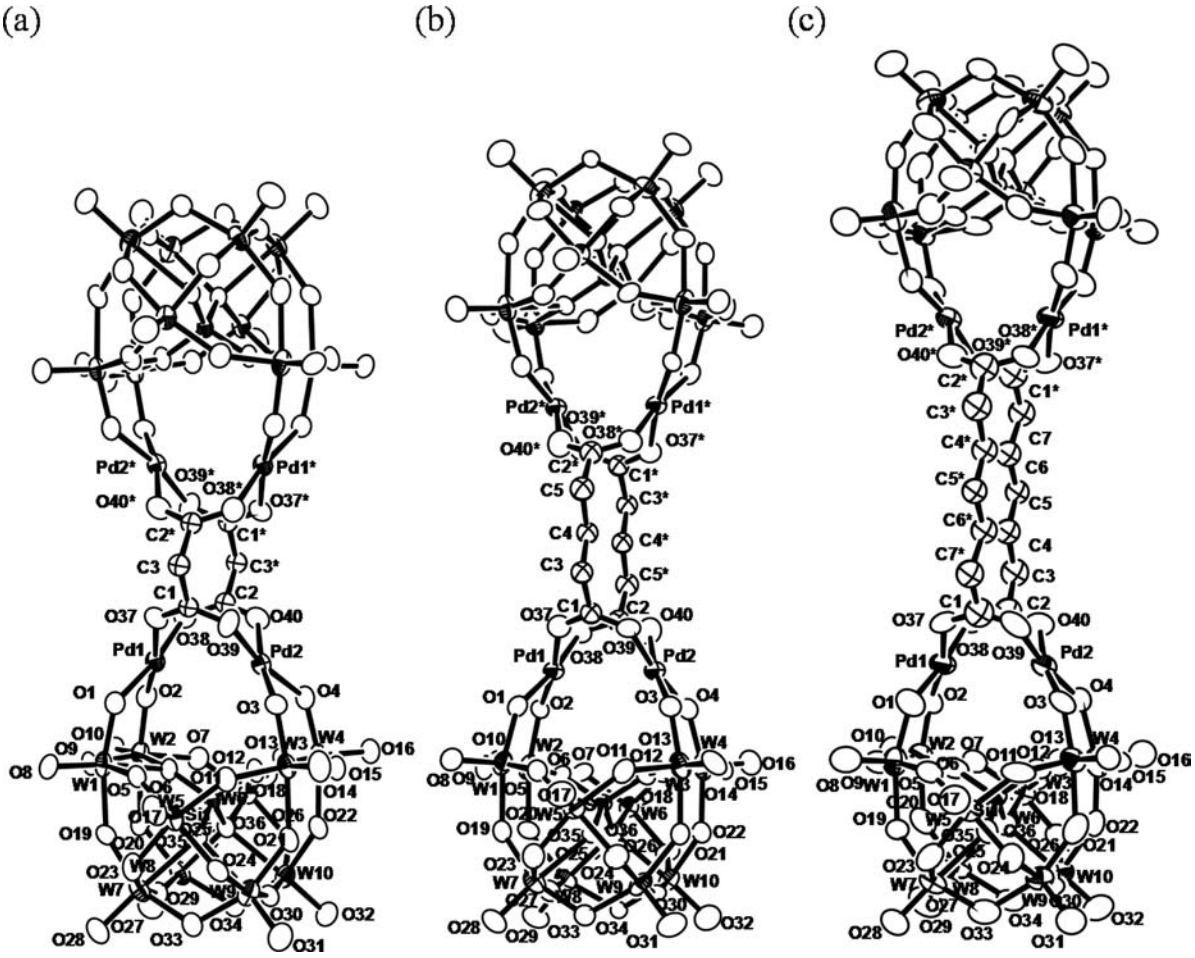

Figure 1. ORTEP drawings of the anion parts of (a) **II**, (b) $\mathbf{III_A}$, and (c) $\mathbf{IV_A}$ drawn at 50% probability level.

solvent molecules could not crystallographically be determined. Two Pd atoms were retained at the lacunary sites of $[\gamma\text{-}SiW_{10}O_{36}]^{8-}$ and in a square-planar arrangement: Each Pd atom was coordinated by two oxygen atoms of $[\gamma\text{-}SiW_{10}O_{36}]^{8-}$ and bridged with two carboxylate ligands. The bond valence sum (BVS) values of palladium (2.26−2.44), tungsten (5.90−6.77), and silicon (3.97−4.00) indicate that respective valences are +2, +6, and +4. The BVS values of oxygen atoms suggest that four oxygen atoms of cyclic dimers are monoprotonated: In the case of **II**, the BVS values of O21 (or O21*) and O22 (or O22*) were 1.49 and 1.45, respectively, and lower than those (1.56−2.13) of the other oxygen atoms, suggesting that O21, O21*, O22, and O22* are monoprotonated.[8] Therefore, the formulas of the cyclic dimers can be described as $TBA_8[\{(\gamma\text{-}H_2SiW_{10}O_{36}Pd_2)(O_2C(CH_2)_nCO_2)\}_2]$ (n = 1 (**II**), 3 (**III**), and 5 (**IV**)). The sums of O−Pd−O angles of **II** (358−359°), **III** (358−359°), and **IV** (358−359°) were very close to 360°. The Pd−O bond lengths of **II** (1.96−2.01 Å), **III** (1.98−2.02 Å), and **IV** (1.94−2.01 Å) were close to those (1.96−2.03 Å) of $TPeA_4[\gamma\text{-}H_2SiW_{10}O_{36}Pd_2(OAc)_2]$ ($\mathbf{I_{TPeA}}$, TPeA = $[(n\text{-}C_5H_{11})_4N]^+$).[6] These results suggest that structures of dipalladium-substituted γ-Keggin silicodecatungstate units, $[\gamma\text{-}H_2SiW_{10}O_{36}Pd_2(O_2C)_2]$, of **II**, **III**, and **IV** are essentially isomorphous to that of $\mathbf{I_{TBA}}$. The IR spectra of cyclic dimers showed the asymmetric (1615 (**II**), 1587 (**III**), and 1585 cm^{-1} (**IV**)) and symmetric (1355 (**II**), 1411 (**III**), and 1411 cm^{-1} (**IV**)) stretching vibration bands of carboxylate groups (Figure S2 in the Supporting Information). The $\Delta(\nu_{asym}(COO^-) - \nu_{sym}(COO^-))$ values of **III** (176 cm^{-1}) and **IV** (174 cm^{-1}) were very close to those of $\mathbf{I_{TBA}}$ (166 cm^{-1}) and palladium complexes with bridging bidentate ligands (116−173 cm^{-1}).[9] The large Δ value (260 cm^{-1}) of **II** would result from an interaction between the coordinated carboxylate groups of the same malonate ligand.[10]

One-pot synthesis of **II**, **III**, and **IV** could be achieved by the stepwise reactions of $TBA_4[\gamma\text{-}SiW_{10}O_{34}(H_2O)_2]$ (TBA·SiW10), $Pd(OAc)_2$, and the corresponding dicarboxylic acids (see the Supporting Information).[11] Pope and co-workers reported that ligand exchange of acetate ligands in a dichromium-substituted γ-Keggin silicodecatungstate, $[\gamma\text{-}SiW_{10}O_{36}(OH)\text{-}Cr_2(OAc)_2(OH_2)_2]^{5-}$, with oxalate ligands was unsuccessful.[5k] *The synthesis of POM-based hybrids by the use of ligand exchange of acetate ligands in TMSPs has never been reported.*[12,13]

The lengths between two POMs (the lengths between two carboxyl oxygen atoms) increased with increase in methylene chain lengths in the order of **II** (3.3 Å) < **III** (5.8 Å) < **IV** (8.2 Å), and the differences (ca. 2.4−2.5 Å) correspond to the lengths of two methylene groups. The cold spray ionization mass (CSI-MS) spectra of TBA salts of the hybrids in DCE exhibited +1-charged peaks (centered at m/z = 7701 (**II**), 7757 (**III**), and 7813 (**IV**)) and +2-charged peaks (centered at m/z = 3972 (**II**), 4000 (**III**), and 4028 (**IV**)) with isotopic distributions that agreed with the patterns calculated for $TBA_9[\{(H_2SiW_{10}O_{36}Pd_2)(O_2C(CH_2)_nCO_2)\}_2]^+$ and $TBA_{10}[\{(H_2SiW_{10}O_{36}Pd_2)(O_2C(CH_2)_nCO_2)\}_2]^{2+}$ (n = 1, 3, 5), respectively (Figure 2). The +1-charged peaks differ by 56

dx.doi.org/10.1021/ic302703k | *Inorg. Chem.* 2013, 52, 2662−2670

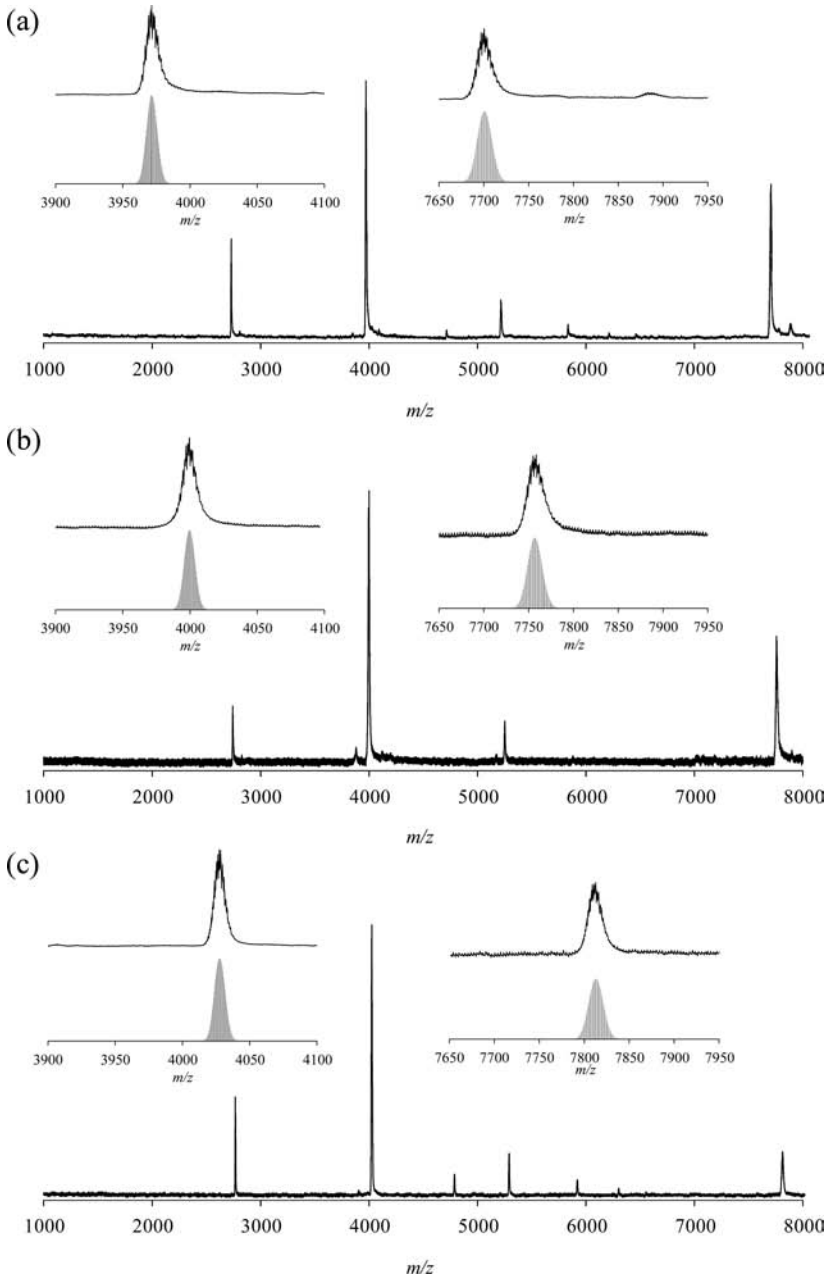

Figure 2. Positive ion CSI-MS spectra (m/z = 1000−8000) of (a) **II**, (b) **III**, and (c) **IV** in DCE. Inset: Positive ion CSI-MS spectra (m/z = 3900−4100 and 7650−7950) (top) and the calculated patterns of $TBA_{10}[\{(H_2SiW_{10}O_{36}Pd_2)(O_2C(CH_2)_nCO_2)\}_2]^{2+}$ (n = (a) 1, (b) 3, and (c) 5) and $TBA_9[\{(H_2SiW_{10}O_{36}Pd_2)(O_2C(CH_2)_nCO_2)\}_2]^{+}$, ($n$ = (a) 1, (b) 3, and (c) 5), respectively (bottom).

mass units which correspond to those of four methylene groups.

The solution state of **II** was investigated by ^{1}H, ^{13}C{H}, and ^{29}Si NMR spectroscopies (Table 3 and Figures S3−S5 in the Supporting Information). The ^{29}Si NMR spectrum of **II** in nitromethane-d_3/acetone-d_6 (11/3, v/v) in the presence of 20 equiv of D_2O with respect to **II** showed one signal at −85.5 ppm, showing the presence of the single species.[14,15] The ^{1}H NMR spectrum of **II** showed a signal at 2.71 ppm assignable to methylene protons of malonate ligands. The ^{13}C{H} NMR spectrum of **II** showed signals at 48.3 and 183.3 ppm assignable to methylene and carbonyl carbons of malonate ligands, respectively. These results suggest that the solid state structure of **II** is maintained in the solution state. The solution states of **III** and **IV** were also investigated by ^{1}H and ^{13}C{H} NMR spectroscopies. The ^{1}H and ^{13}C{H} NMR spectra of **III** and **IV** showed signals of the corresponding dicarboxylate ligands in the hybrids. Detection of the hybrids by ^{183}W NMR spectroscopy was unsuccessful because the solubility in the solvent was low and the quantity was below the detection limit of ^{183}W nuclei.

Reversible Structure Transformation of IV during DCE Sorption−Desorption. All the DCE molecules in $\mathbf{IV_A}$ could crystallographically be determined, and these DCE molecules were easily desorbed at atmospheric pressure and 295 K.[16] The structure transformation of POM-based compounds concomitant with desorption of a large amount of solvent molecules has scarcely been reported.[17] Therefore, the structure transformation of $\mathbf{IV_A}$ was investigated during DCE sorption−desorption. The DCE sorption−desorption properties of $\mathbf{IV_B}$

dx.doi.org/10.1021/ic302703k | Inorg. Chem. 2013, 52, 2662−2670

Table 3. NMR Parameters of II, III, and IV[a]

		chemical shift (ppm)		
entry	compound	^{1}H	^{13}C{^{1}H}	^{29}Si
1	**II**	2.71	48.3, 183.3	−85.5 ($\Delta\nu_{1/2}$ = 20 Hz)
2[b]	**III**	1.17, 1.76[c] (with the respective intensity ratio of 1:2)	36.3, 190.9	not measured[d]
3	**IV**	0.60, 1.14, 1.97 (with the respective intensity ratio of 1:2:2)	27.4, 28.8, 37.5, 191.2	not measured[d]

[a]NMR spectra were measured at 248 K. The ^{1}H NMR signals at 3.37, 1.77, 1.46, and 0.99 ppm and ^{13}C{H} NMR signals at 59.2, 24.5, 20.6, and 14.2 ppm are assignable to TBA. [b]The ^{13}C{H} NMR signal of central methylene carbon in glutarate ligands would be overlapped with that of TBA. [c]The signal at 1.76 ppm was overlapped with that of TBA. [d]The ^{29}Si NMR spectra were not measured because of the low solubilities of **III** and **IV** in the mixed solvent (ref 14).

($\mathbf{IV_B}$: **IV** with 0.2DCE), which was prepared by the evacuation of $\mathbf{IV_A}$ at 298 K for 5 h, were investigated (Figure 3). The DCE

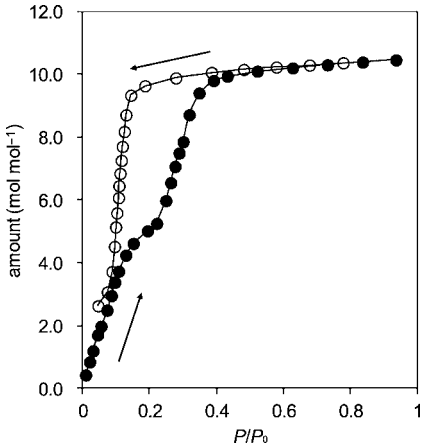

Figure 3. DCE sorption−desorption isotherms of $\mathbf{IV_B}$ at 298 K. Closed and open symbols indicate the sorption and desorption branches, respectively.

sorption isotherm consisted of two steps. The saturated amount of DCE sorbed was 10.5 mol mol^{-1}, and the value was close to the amount (10 mol mol^{-1}) of crystallographically assigned DCE molecules.[18,19] The amount of DCE was also confirmed by ^{1}H NMR spectroscopy. The surface area of $\mathbf{IV_B}$ as calculated with the Brunauer−Emmett−Teller (BET) plot of the N_2 adsorption isotherm at 77 K was 1.4 m^2 g^{-1}. Therefore, the amount (10.5 mol mol^{-1}) of DCE sorbed was 2 orders of magnitude larger than that of the surface adsorption (ca. 6.2 × 10^{-2} mol mol^{-1}), showing the sorption of DCE into the bulk of $\mathbf{IV_B}$. The sorption−desorption isotherms showed a large hysteresis that extended to the lower relative pressure, which would be explained by the specific host−guest interaction.[20] As mentioned above, all DCE molecules in $\mathbf{IV_A}$ were present in the vicinity of polyanions (Figure S6 in the Supporting Information). The distances between the carbon atoms of DCE and the nearest-neighboring oxygen atoms of polyanions were 3.1−3.4 Å, suggesting that DCE molecules interact with polyanions via hydrogen-bonding (Table S4 in the Supporting Information). Such specific interactions between DCE molecules and polyanions led to the low-pressure hysteresis.[21]

By the exposure of $\mathbf{IV_B}$ to saturated DCE vapor, the powder XRD pattern showed good agreement with the calculated one using single-crystal data of $\mathbf{IV_A}$ (Figures 4 (a−b)).[22,23] The structure transformation was investigated by in situ powder XRD measurements under DCE vapor (Figure 4). After the measurement of $\mathbf{IV_B}$ under saturated DCE vapor, the relative DCE vapor pressure was gradually decreased to P/P_0 = 0.0. The powder XRD patterns remained almost unchanged in the range of $P/P_0 \geq 0.2$, while changes were observed with further decrease in the relative DCE vapor pressure, and $\mathbf{IV_C}$ ($\mathbf{IV_C}$: **IV** with 0.7DCE) was formed at P/P_0 = 0.0 (i.e., by the treatment in a dry N_2 at 303 K for 12 h) (Figures 4 (c−h)).[24] These in situ powder XRD results were consistent with the desorption plots with a sudden decrease around P/P_0 = 0.15. The crystal structure of $\mathbf{IV_C}$ was solved by the powder XRD pattern analysis (Figure S8 in the Supporting Information). The structure was constructed in the same space group of $\mathbf{IV_A}$ (*Pbca*) with an optimized unit cell parameter of a = 28.12 Å, b = 26.66 Å, and c = 29.43 Å (Table 4). All the lattice lengths decreased from those of $\mathbf{IV_A}$ (a = 30.04 Å, b = 28.77 Å, c = 30.11 Å). The arrangement of polyanions along the c axis was slightly changed from that of $\mathbf{IV_A}$, while those along the a and b axes were almost the same as those of $\mathbf{IV_A}$ (Figure S9 in the Supporting Information). The TBA cations were uniformly distributed in the crystal lattice.[25] The space filling model of $\mathbf{IV_C}$ and N_2 adsorption isotherms (77 K) showed that $\mathbf{IV_C}$ was nonporous (Figure S10 in the Supporting Information). The powder XRD pattern of $\mathbf{IV_A}$ was restored by the exposure of $\mathbf{IV_C}$ to saturated DCE vapor (Figure 4(i)). The decrease of the relative DCE vapor pressure led to the formation of $\mathbf{IV_C}$ again (Figure 4(j)), suggesting the reversible structure change between $\mathbf{IV_A}$ and $\mathbf{IV_C}$.

All these results of DCE sorption−desorption isotherms and in situ powder XRD measurements suggest the reversible structure transformation between $\mathbf{IV_A}$ and $\mathbf{IV_C}$ driven by DCE sorption−desorption. The flexibility of **IV** would allow DCE molecules to diffuse into the bulk solid, and all DCE molecules can interact with polyanions via hydrogen-bonding, resulting in the reversible structure transformation during DCE sorption−desorption.[26]

CONCLUSION

In summary, inorganic-organic-inorganic hybrids of dipalladium-substituted γ-Keggin silicodecatungstates (**II**, **III**, and **IV**) were synthesized by ligand exchange of the acetate ligands in $\mathbf{I_{TBA}}$ with the corresponding dicarboxylic acids, and the crystal structures were successfully determined. The lengths of organic linker units could precisely be controlled by selecting appropriate dicarboxylate ligands. One-pot synthesis of these hybrids could be achieved by the stepwise reactions of TBA·SiW10, $Pd(OAc)_2$, and dicarboxylic acids. The reversible structure transformation between $\mathbf{IV_A}$ and $\mathbf{IV_C}$ driven by DCE sorption−desorption was confirmed by in situ powder XRD measurements under DCE vapor. The structural flexibility would allow the DCE molecules to diffuse into the bulk solid.

EXPERIMENTAL SECTION

Materials. $Pd(OAc)_2$ (Aldrich), tetra-*n*-butylammonium bromide (TCI), acetone (Kanto Chemical), diethyl ether (Kanto Chemical), 1,2-dichloroethane (Kanto Chemical), $Na_2WO_4{\cdot}2H_2O$ (Nippon Inorganic Color & Chemical), $Na_2SiO_3{\cdot}9H_2O$ (Wako Chemical), KCl (Nacalai Tesque), and dicarboxylic acids (TCI or Wako Chemical) were purchased and used as received.

dx.doi.org/10.1021/ic302703k | Inorg. Chem. 2013, 52, 2662−2670

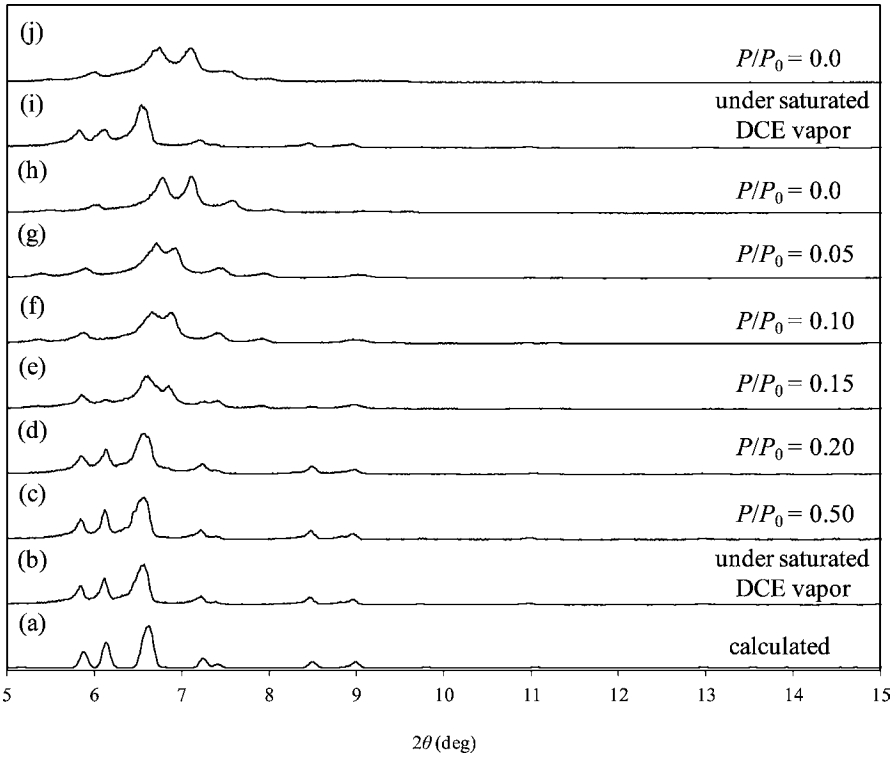

Figure 4. (a) Calculated powder XRD pattern using single-crystal data of $\mathbf{IV_A}$ measured at 293 K. (b–j) Powder XRD patterns of $\mathbf{IV_B}$ under various relative DCE vapor pressures at 303 K. (b) $\mathbf{IV_A}$ ($\mathbf{IV_B}$ exposed to saturated DCE vapor), (c–g) $\mathbf{IV_A}$ (phase (b)) with decrease in the relative DCE pressure to P/P_0 = 0.05, (h) $\mathbf{IV_C}$, (i) $\mathbf{IV_C}$ exposed to saturated DCE vapor, and (j) $\mathbf{IV_A}$ (phase (i)) treated under dry N_2. The relative DCE vapor pressure was controlled with N_2 balance.

Table 4. Lattice Parameters of $\mathbf{IV_A}$, $\mathbf{IV_B}$, and $\mathbf{IV_C}$

	$\mathbf{IV_A}$ (IV with 10DCE)[a]	$\mathbf{IV_B}$ (IV with 0.2DCE)[b]	$\mathbf{IV_C}$ (IV with 0.7DCE)
crystal system	orthorhombic	orthorhombic	orthorhombic
space group	*Pbca* (No. 61)	*Pbca* (No. 61)	*Pbca* (No. 61)
a (Å)	30.0423(4)	27.33	28.12
b (Å)	28.7748(3)	25.86	26.66
c (Å)	30.1121(4)	28.34	29.43
V (Å^3)	26030.7(6)	20029	22057
temp. (K)	293	303	303
Rp		0.1127	0.1257
Rwp		0.1038	0.0798

[a]The detailed crystallographic data for $\mathbf{IV_A}$ (at 293 K) are shown in Table S3 of the Supporting Information. [b]Lattice parameters calculated by Pawley refinement.

Instruments. IR spectra were measured on a Jasco FT/IR-4100 spectrometer using KBr disks. NMR spectra were recorded on a JEOL ECA-500 spectrometer (^{1}H, 495.1 MHz; ^{13}C, 124.50 MHz; ^{29}Si, 98.37 MHz) by using 5 mm tubes. Chemical shifts (δ) were reported in parts per million (ppm) downfield from $SiMe_4$ (solvent, $CDCl_3$) for ^{1}H, ^{13}C{H}, and ^{29}Si NMR spectra. CSI-MS spectra were recorded on a JEOL JMS-T100-CS spectrometer. All the CSI-MS measurements were completed within 10 min. Typical measurements were as follows: Orifice voltage 85 V for positive ions; sample flow 0.1 mL min^{-1}; solvent DCE; concentration 0.1 mM; spray temperature at 263 K; ion source at room temperature. The ICP-AES analyses were performed with Shimadzu ICPS-8100. The elemental analysis was carried out after evacuation of the compounds at room temperature for 5 h, and the amount of solvent molecules was determined by ^{1}H NMR. X-ray diffraction measurements were made on a Rigaku AFC-10 Saturn 724 CCD detector with graphite monochromated Mo Kα radiation (λ = 0.71069 Å). The data of **II** and $\mathbf{III_A}$ were collected using CrystalClear[27] at 183 and 153 K, respectively. The data of $\mathbf{IV_A}$ were collected using CrystalClear[27] at 123 and 293 K. Indexing, integration, and absorption correction were performed with HKL2000[28] software for Linux. Neutral scattering factors were obtained from the standard source. In the data reduction, corrections for Lorentz and polarization effects were made. The structural analysis was performed using CrystalStructure[29] and Win-GX for Windows software.[30] The molecular structures of **II**, $\mathbf{III_A}$, and $\mathbf{IV_A}$ were solved with SHELXS-97 (direct methods) and SHELXH-97 (Fourier and least-squares refinement).[31] Palladium, tungsten, silicon, and oxygen atoms were refined anisotropically, and carbon and nitrogen atoms were refined isotropically. Hydrogen atoms were not included in the calculation. For **II** and $\mathbf{III_A}$, the highly disordered solvent of crystallization (acetone or DCE) was omitted by use of SQUEEZE program.[32] Detailed crystallographic data for **II**, $\mathbf{III_A}$, and $\mathbf{IV_A}$ (at 123 K) are summarized in Table 1. Detailed crystallographic data for $\mathbf{IV_A}$ (at 293 K) are summarized in Table S3 of the Supporting Information. Selected bond lengths and angles for **II**, $\mathbf{III_A}$, and $\mathbf{IV_A}$ (at 123 K) are shown in Table 2. As for **II**, the disordered atom sets were (C104; C154), (C107, C108; C157, C158), (C110, C111, C112; C160, C161, C162), (C116; C166), (C204; C254), (C213, C214, C215, C216; C263, C264, C265, C266), (C313, C314, C315, C316; C363, C364, C365, C366), (C403, C404; C453, C454), (C407, C408; C457, C458), (C409, C410, C411, C412; C459, C460, C461, C462), and (C415, C416; C465, C466), respectively. The corresponding occupancies were (0.46; 0.54), (0.37; 0.63), (0.73; 0.27), (0.62; 0.238), (0.87; 0.13), (0.41; 0.59), (0.47; 0.53), (0.35; 0.65), (0.66; 0.34), (0.53; 0.47), and (0.43; 0.57). As for $\mathbf{III_A}$, the disordered atom sets were (C108; C158), (C212; C262), (C216; C266), (C315, C316; C365, C366), (C404; C454), (C408; C458), (C409, C410, C411, C412; C459, C460, C461, C462), (C413, C414, C415, C416; C463, C464, C465, C466), (C504; C554), (C508; C558), (C510, C511, C512; C560, C561, C562), (C515, C516; C565, C566), (C608; C658), (C611, C612; C661, C662), (C704; C754), (C705, C706,

dx.doi.org/10.1021/ic302703k | Inorg. Chem. 2013, 52, 2662–2670

C707, C708; C755, C756, C757, C758), (C711, C712; C761, C762), (C714, C715, C716; C764, C765, C766), (C804; C854), (C808; C858), and (C811, C812; C861, C862), respectively. The corresponding occupancies were (0.56; 0.44), (0.46; 0.54), (0.29; 0.71), (0.47; 0.53), (0.36; 0.64), (0.26; 0.74), (0.46; 0.54), (0.47; 0.53), (0.75; 0.25), (0.25; 0.75), (0.64; 0.36), (0.78; 0.22), (0.51; 0.49), (0.51; 0.49), (0.31; 0.69), (0.55; 0.45), (0.52; 0.48), (0.43; 0.57), (0.72; 0.28), (0.60; 0.40), and (0.68; 0.32). As for $\mathbf{IV_A}$, the disordered atom sets were (Cl4; Cl54), (Cl7; Cl57), (Cl8; Cl58), (Cl9; Cl59), (C303, C304; C353, C354), (C308; C358), (C403, C404; C453, C454), (C406, C407, C408; C456, C457, C458), and (C413, C414, C415, C416; C463, C464, C465, C466), respectively. The corresponding occupancies were (0.41; 0.59), (0.62; 0.38), (0.74; 0.26), (0.83; 0.17), (0.76; 0.24), (0.75; 0.25), (0.77; 0.23), (0.64, 0.36), and (0.45; 0.55). The volume of the DCE molecule (131 Å^3) was calculated from the molecular weight and density of the liquid and used for the calculation of the volume of solvent molecules in the crystal structure. The DCE vapor sorption isotherms were measured at 298 K using an automatic volumetric vapor sorption apparatus Belsorp (BEL Japan Inc.). Vapor saturation pressure (P_0) of DCE at 298 K was 10.5 kPa. About 0.1 g of the compounds was evacuated at 298 K for 30 min before the sorption measurement. Powder XRD patterns of $\mathbf{IV_B}$ under a vapor flow of DCE were measured with an XRD-DSCII (Rigaku Corporation) and Cu Kα radiation (λ = 1.54056 Å) at 303 K. The diffraction data were collected in the range of 2θ = 5−25° at 0.01° points and 3 s/step. Before the powder XRD measurement, $\mathbf{IV_B}$ was ground with mortar and pestle for 10 s and exposed to saturated DCE vapor for 26 h. The powder XRD pattern of $\mathbf{IV_B}$ under saturated DCE vapor agreed well with the calculated one obtained with single-crystal data of $\mathbf{IV_A}$. The crystallographic parameters and the positions of polyanions and TBA cations of $\mathbf{IV_C}$ were calculated using Materials Studio Software (Accelrys Inc.) as follows: The unit cell indexing and space group determination were carried out by X-cell.[33] The peak profile fitting was performed by the Pawley refinement.[34] The structures of anion part of $\mathbf{IV_C}$ and a TBA cation were optimized with Gaussian09 and the obtained models were used as input for the Rietveld refinement (see the Supporting Information).[35] The optimization and refinement of the arrangement of polyanions was performed by the simulated annealing method[36] and the Rietveld method,[37] respectively. Then, the positions and conformations of TBA cations were optimized by the simulated annealing method and the Forcite module using the Geometry Optimization routine with the universal force field.[38] Finally, the optimization and refinement of the arrangement of polyanions and TBA cations was performed by the Rietveld method.

Synthesis and Characterization of $[(n\text{-}C_4H_9)_4N]_8[\{(\gamma\text{-}H_2SiW_{10}O_{36}Pd_2)(O_2C(CH_2)CO_2)\}_2]$ (II). To a mixed solvent of acetone and water (4.0/0.1 mL) containing $\mathbf{I_{TBA}}$ (0.1 g, 27 μmol), malonic acid (2.8 mg, 27 μmol) was added. The solution was kept at 278 K for several days, and the yellow crystals of **II** were obtained (39 mg, 39% yield). By stirring the reaction solution for 2 h at room temperature instead of keeping the solution, the yellow powders of analytically pure **II** were obtained in 68% yield. IR (KBr): 2961, 2872, 1615, 1483, 1378, 1355, 1152, 1014, 997, 955, 924, 876, 824, 776, 737, 561, 386, 362 cm^{-1}; positive ion MS (CSI, DCE): m/z: 7701 $TBA_9[\{(H_2SiW_{10}O_{36}Pd_2)(O_2C(CH_2)CO_2)\}_2]^+$, 5836 $TBA_{28}[\{(H_2SiW_{10}O_{36}Pd_2)(O_2C(CH_2)CO_2)\}_6]^{4+}$, 5215 $TBA_{19}[\{(H_2SiW_{10}O_{36}Pd_2)(O_2C(CH_2)CO_2)\}_4]^{3+}$, 3972 $TBA_{10}[\{(H_2SiW_{10}O_{36}Pd_2)(O_2C(CH_2)CO_2)\}_2]^{2+}$, 2729 $TBA_{11}[\{(H_2SiW_{10}O_{36}Pd_2)(O_2C(CH_2)CO_2)\}_2]^{3+}$; elemental analysis calcd (%) for $C_{134}H_{296}N_8O_{80}Pd_4Si_2W_{20}$ ($TBA_8[\{(H_2SiW_{10}O_{36}Pd_2)(O_2C(CH_2)CO_2)\}_2]$): C 21.58, H 4.00, N 1.50, Si 0.75, Pd 5.71, W 49.30; found: C 21.46, H 4.10, N 1.42, Si 0.76, Pd 5.85, W 49.07.

Synthesis and Characterization of $[(n\text{-}C_4H_9)_4N]_8[\{(\gamma\text{-}H_2SiW_{10}O_{36}Pd_2)(O_2C(CH_2)_3CO_2)\}_2]$ (III). Into a mixed solvent of acetone and water (4.0/0.1 mL), $\mathbf{I_{TBA}}$ (0.1 g, 27 μmol) was dissolved. To the solution, glutaric acid (3.6 mg, 27 μmol) was added, and the solution was stirred for 2 h at room temperature. The yellow precipitates (66 mg, 66% yield) were collected by filtration, washed with acetone (12 mL), and evacuated for 30 min at room temperature. The crude precipitates (46 mg) were dissolved into DCE, followed by the addition of diethyl ether. After the solution was left to stand at 278 K for a few days, the resulting yellow crystals of $\mathbf{III_A}$ were obtained (34 mg, 74% yield). IR (KBr): 2961, 2873, 1629, 1587, 1483, 1411, 1381, 1015, 997, 954, 923, 876, 829, 778, 737, 561, 386, 363 cm^{-1}; positive ion MS (CSI, DCE): m/z: 7757 $TBA_9[\{(H_2SiW_{10}O_{36}Pd_2)(O_2C(CH_2)_3CO_2)\}_2]^+$, 5252 $TBA_{19}[\{(H_2SiW_{10}O_{36}Pd_2)(O_2C(CH_2)_3CO_2)\}_4]^{3+}$, 4000 $TBA_{10}[\{(H_2SiW_{10}O_{36}Pd_2)(O_2C(CH_2)_3CO_2)\}_2]^{2+}$, 2747 $TBA_{11}[\{(H_2SiW_{10}O_{36}Pd_2)(O_2C(CH_2)_3CO_2)\}_2]^{3+}$; elemental analysis calcd (%) for $C_{138.2}H_{304.8}Cl_{0.4}N_8O_{80}Pd_4Si_2W_{20}$ ($TBA_8[\{(H_2SiW_{10}O_{36}Pd_2)(O_2C(CH_2)_3CO_2)\}_2]\cdot 0.2DCE$): C 22.06, H 4.08, N 1.49, Si 0.75, Pd 5.65, W 48.80; found: C 21.94, H 4.29, N 1.24, Si 0.76, Pd 5.72, W 48.78.

Synthesis and Characterization of $[(n\text{-}C_4H_9)_4N]_8[\{(\gamma\text{-}H_2SiW_{10}O_{36}Pd_2)(O_2C(CH_2)_5CO_2)\}_2]$ (IV). Into a mixed solvent of acetone and water (4.0/0.1 mL), $\mathbf{I_{TBA}}$ (0.1 g, 27 μmol) was dissolved. To the solution, pimelic acid (4.3 mg, 27 μmol) was added, and the solution was stirred for 2 h at room temperature. The yellow precipitates (54 mg, 53% yield) were collected by filtration, washed with acetone (12 mL), and evacuated for 30 min at room temperature. The crude precipitates (15 mg) were dissolved into DCE, followed by the addition of diethyl ether. After the solution was left to stand at 278 K for a few days, the yellow crystals of $\mathbf{IV_A}$ ($\mathbf{IV_A}$: **IV** with 10DCE) were obtained. By the evacuation of $\mathbf{IV_A}$ at 298 K for 5 h, $\mathbf{IV_B}$ ($\mathbf{IV_B}$: **IV** with 0.2DCE) was obtained (12 mg, 75% yield). IR (KBr): 2960, 2872, 1634, 1585, 1483, 1411, 1383, 1015, 997, 954, 923, 876, 829, 780, 736, 561, 386, 362 cm^{-1}; positive ion MS (CSI, DCE): m/z: 7813 $TBA_9[\{(H_2SiW_{10}O_{36}Pd_2)(O_2C(CH_2)_5CO_2)\}_2]^+$, 5920 $TBA_{28}[\{(H_2SiW_{10}O_{36}Pd_2)(O_2C(CH_2)_5CO_2)\}_6]^{4+}$, 5289 $TBA_{19}[\{(H_2SiW_{10}O_{36}Pd_2)(O_2C(CH_2)_5CO_2)\}_4]^{3+}$, 4784 $TBA_{29}[\{(H_2SiW_{10}O_{36}Pd_2)(O_2C(CH_2)_5CO_2)\}_6]^{5+}$, 4028 $TBA_{10}[\{(H_2SiW_{10}O_{36}Pd_2)(O_2C(CH_2)_5CO_2)\}_2]^{2+}$, 2766 $TBA_{11}[\{(H_2SiW_{10}O_{36}Pd_2)(O_2C(CH_2)_5CO_2)\}_2]^{3+}$; elemental analysis calcd (%) for $C_{142.4}H_{312.8}Cl_{0.4}N_8O_{80}Pd_4Si_2W_{20}$ ($TBA_8[\{(H_2SiW_{10}O_{36}Pd_2)(O_2C(CH_2)_5CO_2)\}_2]\cdot 0.2DCE$): C 22.53, H 4.15, N 1.48, Si 0.74, Pd 5.61, W 48.44; found: C 22.29, H 4.20, N 1.37, Si 0.74, Pd 5.61, W 48.94.

■ ASSOCIATED CONTENT

Supporting Information

Experimental details, X-ray crystallographic data in CIF format for **II**, $\mathbf{III_A}$, and $\mathbf{IV_A}$, Tables S1−S4, and Figures S1−S10. This material is available free of charge via the Internet at http://pubs.acs.org.

■ AUTHOR INFORMATION

Corresponding Author

*Phone: +81-3-5841-7272. Fax: +81-3-5841-7220. E-mail: tmizuno@mail.ecc.u-tokyo.ac.jp.

Present Address

†Department of Basic Sciences, School of Arts and Sciences, The University of Tokyo, 3-8-1 Komaba, Meguro-ku, Tokyo 153-8902, Japan.

Notes

The authors declare no competing financial interest.

■ ACKNOWLEDGMENTS

This work was supported in part by the Japan Society for the Promotion of Science (JSPS) through its "Funding Program for World-Leading Innovative R&D on Science and Technology (FIRST Program)", and Grants-in-Aid for Scientific Research from the Ministry of Education, Culture, Science, Sports, and Technology of Japan. T.H. is grateful for a JSPS Research Fellowship for Young Scientists.

REFERENCES

(1) (a) Sanchez, C.; Soler-Illia, G. J. de A. A.; Ribot, F.; Lalot, T.; Mayer, C. R.; Cabuil, V. *Chem. Mater.* **2001**, *13*, 3061−3083. (b) Wang, M.-S.; Xu, G.; Zhang, Z.-J.; Guo, G.-C. *Chem. Commun.* **2010**, *46*, 361−376. (c) Descalzo, A. B.; Martínez-Máñez, R.; Sancenón, F.; Hoffmann, K.; Rurack, K. *Angew. Chem., Int. Ed.* **2006**, *45*, 5924−5948. (d) Sanchez, C.; Julián, B.; Belleville, P.; Popall, M. *J. Mater. Chem.* **2005**, *15*, 3559−3592.

(2) (a) Pope, M. T. *Heteropoly and Isopoly Oxometalates*; Springer-Verlag: Berlin, Germany, 1983. (b) Thematic issue on POMs. Hill, C. L. *Chem. Rev.* **1998**, *98*, 1−390. (c) Dolbecq, A.; Dumas, E.; Mayer, C. R.; Mialane, P. *Chem. Rev.* **2010**, *110*, 6009−6048. (d) Proust, A.; Thouvenot, R.; Gouzerh, P. *Chem. Commun.* **2008**, 1837−1852. (e) Song, Y.-F.; Long, D.-L.; Ritchie, C.; Cronin, L. *Chem. Rec.* **2011**, *11*, 158−171.

(3) (a) Song, Y.-F.; Tsunashima, R. *Chem. Soc. Rev.* **2012**, *41*, 7384−7402. (b) Long, D.-L.; Tsunashima, R.; Cronin, L. *Angew. Chem., Int. Ed.* **2010**, *49*, 1736−1758. (c) Li, D.; Yin, P.; Liu, T. *Dalton Trans.* **2012**, *41*, 2853−2861. (d) Proust, A.; Matt, B.; Villanneau, R.; Guillemot, G.; Gouzerh, P.; Izzet, G. *Chem. Soc. Rev.* **2012**, *41*, 7605−7622. (e) Liu, S.; Möhwald, H.; Volkmer, D.; Kurth, D. G. *Langmuir* **2006**, *22*, 1949−1951. (f) Gatard, S.; Blanchard, S.; Schollhorn, B.; Gouzerh, P.; Proust, A.; Boubekeur, K. *Chem.—Eur. J.* **2010**, *16*, 8390−8399. (g) Landsmann, S.; Lizandara-Pueyo, C.; Polarz, S. *J. Am. Chem. Soc.* **2010**, *132*, 5315−5321. (h) Yin, P.; Wu, P.; Xiao, Z.; Li, D.; Bitterlich, E.; Zhang, J.; Cheng, P.; Vezenov, D. V.; Liu, T.; Wei, Y. *Angew. Chem., Int. Ed.* **2011**, *50*, 2521−2525.

(4) (a) Pradeep, C. P.; Misdrahi, M. F.; Li, F.-Y.; Zhang, J.; Xu, L.; Long, D.-L.; Liu, T.; Cronin, L. *Angew. Chem., Int. Ed.* **2009**, *48*, 8309−8313. (b) Pradeep, C. P.; Li, F.-Y.; Lydon, C.; Miras, H. N.; Long, D.-L.; Xu, L.; Cronin, L. *Chem.—Eur. J.* **2011**, *17*, 7472−7479. (c) Misdrahi, M. F.; Wang, M.; Pradeep, C. P.; Li, F.-Y.; Lydon, C.; Xu, L.; Cronin, L.; Liu, T. *Langmuir* **2011**, *27*, 9193−9202. (d) Li, Q.; Wei, Y.; Hao, J.; Zhu, Y.; Wang, L. *J. Am. Chem. Soc.* **2007**, *129*, 5810−5811. (e) Stark, J. L.; Rheingold, A. L.; Maatta, E. A. *J. Chem. Soc., Chem. Commun.* **1995**, 1165−1166. (f) Zhu, Y.; Wang, L.; Hao, J.; Xiao, Z.; Wei, Y.; Wang, Y. *Cryst. Growth Des.* **2009**, *9*, 3509−3518. (g) Lu, M.; Wei, Y.; Xu, B.; Cheung, C. F.-C.; Peng, Z.; Powell, D. R. *Angew. Chem., Int. Ed.* **2002**, *41*, 1566−1568. (h) Mayer, C. R.; Hervé, M.; Lavanant, H.; Blais, J.-C.; Sécheresse, F. *Eur. J. Inorg. Chem.* **2004**, 973−977. (i) Rousseau, G.; Rivière, E.; Dolbecq, A.; Marrot, J.; Oms, O.; Mialane, P. *Eur. J. Inorg. Chem.* DOI: 10.1002/ejic.201201012.

(5) (a) Godin, B.; Chen, Y. G.; Vaissermann, J.; Ruhlmann, L.; Verdaguer, M.; Gouzerh, P. *Angew. Chem., Int. Ed.* **2005**, *44*, 3072−3075. (b) Wang, J.-P.; Ma, P.-T.; Li, J.; Niu, H.-Y.; Niu, J.-Y. *Chem.—Asian J.* **2008**, *3*, 822−833. (c) Mialane, P.; Dolbecq, A.; Sécheresse, F. *Chem. Commun.* **2006**, 3477−3485. (d) Fang, X.; Kögerler, P. *Chem. Commun.* **2008**, 3396−3398. (e) Lisnard, L.; Mialane, P.; Dolbecq, A.; Marrot, J.; Clemente-Juan, J. M.; Coronado, E.; Keita, B.; de Oliveira, P.; Nadjo, L.; Sécheresse, F. *Chem.—Eur. J.* **2007**, *13*, 3525−3536. (f) Botar, B.; Ellern, A.; Kögerler, P. *Dalton Trans.* **2009**, 5606−5608. (g) Errington, R. J.; Petkar, S. S.; Middleton, P. S.; McFarlane, W.; Clegg, W.; Coxall, R. A.; Harrington, R. W. *J. Am. Chem. Soc.* **2007**, *129*, 12181−12196. (h) Assran, A. S.; Mal, S. S.; Izarova, N. V.; Banerjee, A.; Suchopar, A.; Sadakane, M.; Kortz, U. *Dalton Trans.* **2011**, *40*, 2920−2925. (i) Zhang, W.; Liu, S.-X.; Zhang, C.-D.; Tan, R.-K.; Ma, F.-J.; Li, S.-J.; Zhang, Y.-Y. *Eur. J. Inorg. Chem.* **2010**, 3473−3477. (j) Mialane, P.; Dolbecq, A.; Rivière, E.; Marrot, J.; Sécheresse, F. *Eur. J. Inorg. Chem.* **2004**, 33−36. (k) Wassermann, K.; Lunk, H.-J.; Palm, R.; Fuchs, J.; Steinfeldt, N.; Stösser, R.; Pope, M. T. *Inorg. Chem.* **1996**, *35*, 3273−3279. (l) Wei, X.; Dickman, M. H.; Pope, M. T. *Inorg. Chem.* **1997**, *36*, 130−131. (m) Sveshnikov, N. N.; Dickman, M. H.; Pope, M. T. *Inorg. Chim. Acta* **2006**, *359*, 2721−2727. (n) Botar, B.; Kögerler, P.; Hill, C. L. *Inorg. Chem.* **2007**, *46*, 5398−5403. (o) Pichon, C.; Mialane, P.; Dolbecq, A.; Marrot, J.; Rivière, E.; Bassil, B. S.; Kortz, U.; Keita, B.; Nadjo, L.; Sécheresse, F. *Inorg. Chem.* **2008**, *47*, 11120−11128. (p) Chen, L.; Liu, Y.; Chen, S.; Hu, H.; Fu, F.; Wang, J.; Xue, G. *J. Cluster Sci.* **2009**, *20*, 331−340. (q) Kortz, U. *J. Cluster Sci.* **2003**, *14*, 205−214. (r) Al-Kadamany, G.; Mal, S. S.; Milev, B.; Donoeva, B. G.; Maksimovskaya, R. I.; Kholdeeva, O. A.; Kortz, U. *Chem.—Eur. J.* **2010**, *16*, 11797−11800. (s) Hussain, F.; Gable, R. W.; Speldrich, M.; Kögerler, P.; Boskovic, C. *Chem. Commun.* **2009**, 328−330. (t) Niu, J.; Wang, K.; Chen, H.; Zhao, J.; Ma, P.; Wang, J.; Li, M.; Bai, Y.; Dang, D. *Cryst. Growth Des.* **2009**, *9*, 4362−4372. (u) Zheng, S.-T.; Yuan, D.-Q.; Jia, H.-P.; Zhang, J.; Yang, G.-Y. *Chem. Commun.* **2007**, 1858−1860. (v) Fang, X.; Speldrich, M.; Schilder, H.; Cao, R.; O'Halloran, K. P.; Hill, C. L.; Kögerler, P. *Chem. Commun.* **2010**, *46*, 2760−2762. (w) Zhang, D.; Zhang, C.; Chen, H.; Ma, P.; Wang, J.; Niu, J. *Inorg. Chim. Acta* **2012**, *391*, 218−223. (x) Li, D.; Han, H.; Wang, Y.; Wang, X.; Li, Y.; Wang, E. *Eur. J. Inorg. Chem.* DOI: 10.1002/ejic.201200791.

(6) Hirano, T.; Uehara, K.; Kamata, K.; Mizuno, N. *J. Am. Chem. Soc.* **2012**, *134*, 6425−6433.

(7) There were two crystallographically independent anions (**1** and **2**) in the unit cell of $\mathbf{III_A}$, and these structures were almost identical to each other (see Figure S1 in the Supporting Information).

(8) The results of BVS calculations for **II**, $\mathbf{III_A}$, and $\mathbf{IV_A}$ are summarized in Table S2 of the Supporting Information. In the case of $\mathbf{III_A}$, the BVS values of the oxygen atoms (O18 (or O18*), O19 (or O19*), O20 (or O20*), and O32 (or O32*) for **1** (1.58−1.61) and O41 (or O41*), O61 (or O61*), O62 (or O62*) for **2** (1.42−1.46) were lower than those of the other oxygen atoms, suggesting that four protons are disordered over these oxygen atoms. In the case of $\mathbf{IV_A}$, the BVS values of O4 (or O4*) and O19 (or O19*) were 1.34 and 1.39, respectively, and these values were lower than those (1.60−2.27) of the other oxygen atoms, suggesting that O4, O4*, O19, and O19* are monoprotonated.

(9) (a) Deacon, G. B.; Phillips, R. J. *Coord. Chem. Rev.* **1980**, *33*, 227−250. (b) Nakamoto, K. *Infrared Spectra of Inorganic and Coordination Compounds*; Wiley: New York, 1986.

(10) Dziobkowski, C. T.; Wrobleski, J. T.; Brown, D. B. *Inorg. Chem.* **1981**, *20*, 671−678.

(11) Our attempts to synthesize **II** with various palladium salts ($PdCl_2$, $Pd(NO_3)_2$, and $PdSO_4$) instead of $Pd(OAc)_2$ were unsuccessful.

(12) There are only five reports on the synthesis of hybrids by exchange of organic ligands, such as methoxo,[5g,12a,c] *tert*-butoxo,[12a,b] *iso*-propoxo,[12a,d] and trimethylsiloxo[12b] ligands, in TMSPs.[5g] (a) Day, V. W.; Klemperer, W. G.; Schwartz, C. *J. Am. Chem. Soc.* **1987**, *109*, 6030−6044. (b) Radkov, E. V.; Beer, R. H. *Inorg. Chim. Acta* **2000**, *297*, 191−198. (c) Errington, R. J.; Petkar, S. S.; Middleton, P. S.; McFarlane, W.; Clegg, W.; Coxall, R. A.; Harrington, R. W. *Dalton Trans.* **2007**, 5211−5222. (d) Coyle, L.; Middleton, P. S.; Murphy, C. J.; Clegg, W.; Harrington, R. W.; Errington, R. J. *Dalton Trans.* **2012**, *41*, 971−981.

(13) The hydration of benzonitrile in the presence of **II**, **III**, and **IV** under the following reaction conditions: Catalyst (Pd: 25 μmol), benzonitrile (0.5 mmol), DMF (1.0 mL), water (10 mmol), 363 K, 9 h. The hydration of benzonitrile in the presence of **II**, **III**, and **IV** gave benzamide in 91, 81, 93% yields, respectively. The stability of **IV** in the presence of an excess amount of water was investigated by CSI-MS spectroscopy. Upon addition of 13500 equiv of water with respect to **IV** into the acetone solution, the intensity of CSI-MS peaks at m/z = 7813 and 4028 assignable to $TBA_9[\{(H_2SiW_{10}O_{36}Pd_2)(O_2C(CH_2)_5CO_2)\}_2]^+$ and $TBA_{10}[\{(H_2SiW_{10}O_{36}Pd_2)(O_2C(CH_2)_5CO_2)\}_2]^{2+}$, respectively, decreased, and a +1-charged peak centered at m/z = 3904 with isotopic distributions that agreed with the patterns calculated for $TBA_5[H_4SiW_{10}O_{38}Pd_2]^+$ appeared. These results suggest that the pimelate ligands are eliminated by the reaction of **IV** with water to form a monomeric carboxylate-free species and that the species probably plays an important role in the hydration in a similar way to the $\mathbf{I_{TBA}}$-mediated hydration of nitriles.

(14) The solution state of **II** was investigated by ^1H, $^{13}C\{^1H\}$, and ^{29}Si NMR spectroscopies. Among the solvents tested (DCE-d_4, acetone-d_6, acetonitrile-d_3, and nitromethane-d_3), the mixed solution of nitromethane-d_3 and acetone-d_6 in the presence of 20 equiv of D_2O with respect to **II** was used for the NMR measurements because of the following reasons. The ^1H NMR spectrum of **II** in acetonitrile-d_3 showed many unidentified signals. Detection of **II** in DCE-d_4 and

acetone-d_6 by $^{13}C\{^1H\}$ and ^{29}Si NMR spectroscopies was unsuccessful because the solubility of **II** in these solvents was low and the quantity was below the detection limits of ^{13}C and ^{29}Si nuclei. The solution state by the ^{29}Si NMR spectrum of **II** in nitromethane-d_3 showed three signals at −84.9, −85.9, and −86.6 ppm with the respective intensity ratio of 0.3:1.0:0.3. The appearance of extra signals would be caused by ion-pairing interactions (e.g., $H^+\cdots[\{(\gamma\text{-}SiW_{10}O_{36}Pd_2)(O_2C(CH_2)CO_2)\}_2]^{12-}$).[15] Therefore, the NMR spectra of **II** in nitromethane-d_3/acetone-d_6 (11/3, v/v) were measured in the presence of 20 equiv of D_2O with respect to **II** (the mixed solvent was used because nitromethane was not miscible with water). The ^{29}Si NMR spectroscopy was investigated for only **II** because the solubilities of **III** and **IV** in the mixed solvent were much lower than that of **II**.

(15) Finke, R. G.; Rapko, B.; Saxton, R. J.; Domaille, P. J. *J. Am. Chem. Soc.* **1986**, *108*, 2947−2960.

(16) The DCE molecules in $\mathbf{IV_A}$ were easily desorbed at atmospheric pressure and 295 K, and the DCE content decreased to 2.4 molecules per polyanion for 5 min.

(17) The structure transformation of POM-based compounds with desorption of a large amount of organic solvent molecules has scarcely been reported, while there is one report on the structure transformation of $Rb_4[Cr_3O(OOCH)_6(H_2O)_3][BW_{12}O_{40}]\cdot 16H_2O$ with desorption of a large amount of water. Ogasawara, Y.; Uchida, S.; Mizuno, N. *J. Phys. Chem. C* **2007**, *111*, 8218−8227.

(18) The saturated amount of DCE sorbed by $\mathbf{I_{TBA}}$ was 2.9 mol mol^{-1}, and the amount was smaller than that (5.3 mol mol^{-1} (based on the dipalladium-substituted silicodecatungstate unit)) of DCE sorbed by $\mathbf{IV_B}$.

(19) Compound $\mathbf{IV_B}$ also sorbed polar organic molecules, and the amounts of sorption of dichloromethane and 2-propanol at P/P_0 = 0.92 were 12.2 and 6.0 mol mol^{-1}, respectively. These values were much larger than that (0.6 mol mol^{-1}) of water.

(20) Gregg, S. J.; Sing, K. S. W. *Adsorption, Surface Area, and Porosity*; Academic Press: London, U.K., 1982.

(21) The BET surface areas of **II** and $\mathbf{III_A}$ evacuated at 298 K for 5 h were 1.1 and 1.3 $m^2\ g^{-1}$, respectively, and very low. The respective saturated amounts of DCE sorbed were 10.9 and 11.3 mol mol^{-1}, and these amounts were 2 orders of magnitude larger than those of the surface adsorption (4.8×10^{-2} and 5.7×10^{-2} mol mol^{-1}), showing the sorption of DCE into the bulk. In addition, the sorption−desorption isotherms showed large hystereses.

(22) The X-ray diffraction measurement of $\mathbf{IV_A}$ was also performed at 293 K. The space group was the same as that measured at 123 K (orthorhombic, *Pbca*), while the lattice parameters were slightly different from each other (Tables S1 and S3 in the Supporting Information). The powder XRD pattern of $\mathbf{IV_B}$ under saturated DCE vapor was in agreement with the calculated one using the single-crystal data measured at 293 K.

(23) The lattice parameters of $\mathbf{IV_B}$ were calculated by the Pawley method (Figure S7 in the Supporting Information). The structure was constructed in the same space group as that of $\mathbf{IV_A}$ (*Pbca*) with an optimized unit cell parameter of a = 27.33 Å, b = 25.86 Å, and c = 28.34 Å. The decrease in the lattice volume from $\mathbf{IV_A}$ to $\mathbf{IV_B}$ (6002 $Å^3$) was close to the volume of forty DCE molecules (5240 $Å^3$).

(24) In the powder XRD patterns of $\mathbf{IV_C}$ at P/P_0 = 0.2−0.0, the diffraction angles and intensities of the peaks continuously changed. Therefore, an intermediate state between $\mathbf{IV_A}$ and $\mathbf{IV_C}$ would be formed at P/P_0 = 0.15.

(25) The remaining DCE molecules would be present in the voids surrounded by polyanions and TBA cations.

(26) (a) Noro, S.; Tsunashima, R.; Kamiya, Y.; Uemura, K.; Kita, H.; Cronin, L.; Akutagawa, T.; Nakamura, T. *Angew. Chem., Int. Ed.* **2009**, *48*, 8703−8706. (b) Uchida, S.; Kamata, K.; Ogasawara, Y.; Fujita, M.; Mizuno, N. *Dalton Trans.* **2012**, *41*, 9979−9983.

(27) (a) *CrystalClear*, 1.4.0; Rigaku and Rigaku/MSC: The Woodlands, TX, 1999. (b) Pflugrath, J. W. *Acta Crystallogr.* **1999**, *D55*, 1718−1725.

(28) Otwinski, Z.; Minor, W. Processing of X-ray Diffraction Data Collected in Oscillation Mode. In *Methods in Enzymology*; Carter, C. W. Jr., Sweet, R. M., Eds.; Academic Press: New York, 1997; Macromolecular Crystallography, Part A; Vol. *276*, pp 307−326.

(29) *CrystalStructure*, 4.0; Rigaku and Rigaku/MSC: The Woodlands, TX, 2000.

(30) Farrugia, L. J. *J. Appl. Crystallogr.* **1999**, *32*, 837−838.

(31) Sheldrick, G. M. *SHELX97, Programs for Crystal Structure Analysis*, Release 97-2; University of Göttingen: Göttingen, Germany, 1997.

(32) van der Sluis, P.; Spek, L. A. *Acta Crystallogr.* **1990**, *A46*, 194−201.

(33) Neumann, M. A. *J. Appl. Crystallogr.* **2003**, *36*, 356−365.

(34) Pawley, G. S. *J. Appl. Crystallogr.* **1981**, *14*, 357−361.

(35) Frisch, M. J. et al. *Gaussian 09, revision B.01*; Gaussian, Inc.: Wallingford, CT, 2009.

(36) Engel, G. E.; Wilke, S.; König, O.; Harris, K. D. M.; Leusen, F. J. J. *J. Appl. Crystallogr.* **1999**, *32*, 1169−1179.

(37) Rietveld, H. M. *J. Appl. Crystallogr.* **1969**, *2*, 65−71.

(38) Rappé, A. K.; Casewit, C. J.; Colwell, K. S.; Goddard, W. A., III; Skiff, W. M. *J. Am. Chem. Soc.* **1992**, *114*, 10024−10035.